Chemical Vapor Deposition

DOI: 10.1002/cvde.200706655

Full Paper

Growth of Diamond Nanoplatelets by CVD**

By *Hou-Guang Chen,** *Li Chang, Shih-Yin Cho, Jhih-Kun Yan,* and *Chun-An Lu*

Hexagonal, single-crystalline, diamond nanoplatelets synthesized by microwave plasma (MP)CVD on Au-Ge alloy and nanocrystalline diamond (nc-diamond) film substrates, respectively, are reported. On the nc-diamond matrix, hexagonal diamond nanoplatelets can grow to a thickness of as little as approximately 10 nm. The effects of various processing parameters, such as methane concentration, microwave power, and gas pressure, on the growth of diamond nanoplatelets are explored. High-resolution transmission electron microscopy (HRTEM) reveals that the diamond nanoplatelets contain multi-parallel twins, and the side faces of the platelets exhibit {100}/{111} ridge-and-trough structure. Anisotropic growth of diamond nanoplatelet is believed to result from the side face structure of the twinned platelets and intensive plasma reaction.

Keywords: Microstructure, MPCVD, Nanodiamond, TEM, Twinning

1. Introduction

Diamond film growth by CVD has attracted intensive attention in the past two decades, due to its remarkable physical and chemical properties for electronic, mechanical, and biological applications. In addition, diamond with nanometer dimensions, such as nc-diamond films, nanodiamond particles, and colloids have been regarded as a new materials with great potential in various fields such as, biomedical, electronic, and optoelectronic devices.[1–5] In particular, diamond exhibits excellent stability, sensitivity, and selectivity which are necessary factors for biosensor platforms,[4,5] so the development of diamond-based biosensors has experienced heightened interest from various research communities. Moreover, Chao et al. have proposed nanometer-sized diamond particles as a probe for biolabeling.[3] In addition to applications in biology, nanodiamond also has fascinating electron emission properties. The fabrication of stable and robust electron emission cathodes consisting of nc-diamond films, for flat-panel displays or electron beam emitters, has attracted interest from many research groups.[2]

Recently, it has been shown that fabrication of low-dimensional nanostructures (such as nanorods, nanowires, nanosheets, nanoplatelets,...etc.) of diamond material is important for practical nanotechnology applications.[6–9] Some reports have predicted that diamond in nanorod form has unusual mechanical properties.[6] The excellent mechanical properties, such as high elastic modulus and strength-to-weight ratio, are suggested to be the ideal choice for nanometer-size electro-mechanical devices.[5] Several groups attempted to fabricate diamond nanostructures by plasma etching,[10,11] or by growth on anodic aluminum oxide templates.[12] In general, CVD diamonds often exhibit morphologies that are cubo-octahedral or polyhedron. However, the formation of low-dimensional nanostructured diamond by a ''bottom-up'' route is rarely reported. Our previous experiments have shown that unique, two-dimensional, single-crystalline diamond, {111} tabular nanoplatelets or nanosheets in the shape of trapezoids and parallelograms can be deposited on polycrystalline diamond substrates with a Ni-coated layer by high-temperature MPCVD.[9,13] Recently, Lu et al. reported that regular {110} and {111} hexagon diamond nanoplatelets also could be achieved using MPCVD.[14,15] Thus, it verifies that the synthesis of single-crystalline diamond in a low-dimensional nanostructure is feasible.

In this article, we explore further the effects of processing conditions and substrates on the growth of diamond nanoplatelets in MPCVD. We synthesized diamond nanostructures on Au-Ge alloys and nc-diamond substrates. Au-Ge alloy, which is a binary eutectic alloy with a non-carbonization nature, can be in a liquid state at diamond growth temperatures by adjusting the alloy composition, based on the phase diagram. In the past, several studies reported attempts to use liquids as substrates for diamond growth due to extremely high solubility of carbon in the liquid state.[16–18] The high solubility of carbon in the liquid phase would promote diamond nucleation and growth rates during the precipitation of diamond nuclei from carbon-rich alloy liquids. In addition, we also examined the effect of the relative geometric position of the samples in a MP ball on the growth of diamond nanoplatelets by varying the position

[*] Prof. H.-G. Chen
Department of Materials Science and Engineering, I-Shou University Kaohsiung, 840 (Taiwan)
E-mail: houguang@isu.edu.tw
Prof. L. Chang, S.-Y. Cho, Dr. J.-K. Yan, Dr. C.-A. Lu
Department of Materials Science and Engineering, National Chiao Tung University Hsinchu, 300 (Taiwan)

[**] We thank the support from National Science Council, Taiwan, R. O. C. under contract of NSC 95-2221-E-009-089-my3 and NSC 96-2221-E-214-027

Table 1. Process parameters of diamond nanoplatelet growth with various sample placements.

	Microwave power [W]	Growth pressure [Torr]	CH_4 concentration [%] (Total flow rate = 300 sccm)	BEN voltage [V]	Duration [min]	Substrate
Placement I	800	20	4 (BEN stage) 0.667(Growth stage)	−200	15 (BEN stage) 20 (Growth stage)	Au-Ge alloy
Placement II	~800–900	~20–25	~0.667–2	NA	15	nc-diamond
Placement III	1000	~30–70	~1–3	NA	~5–30	nc-diamond

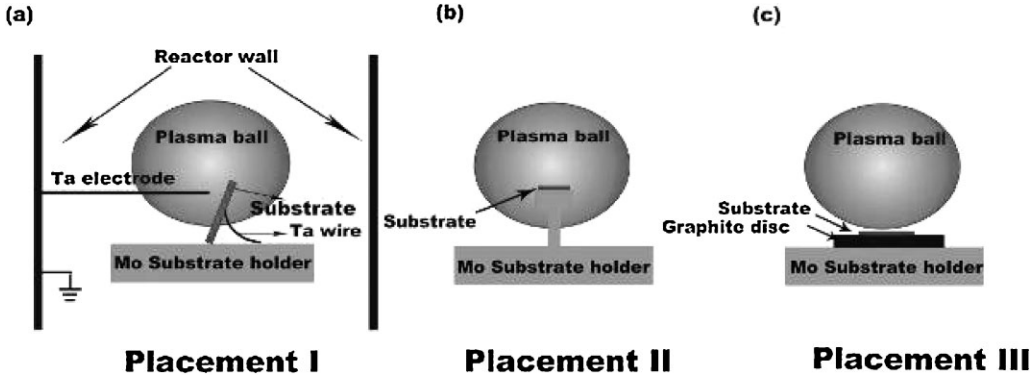

Fig. 1. Schematic illustration of three types of sample placements for the growth of diamond nanoplatelets.

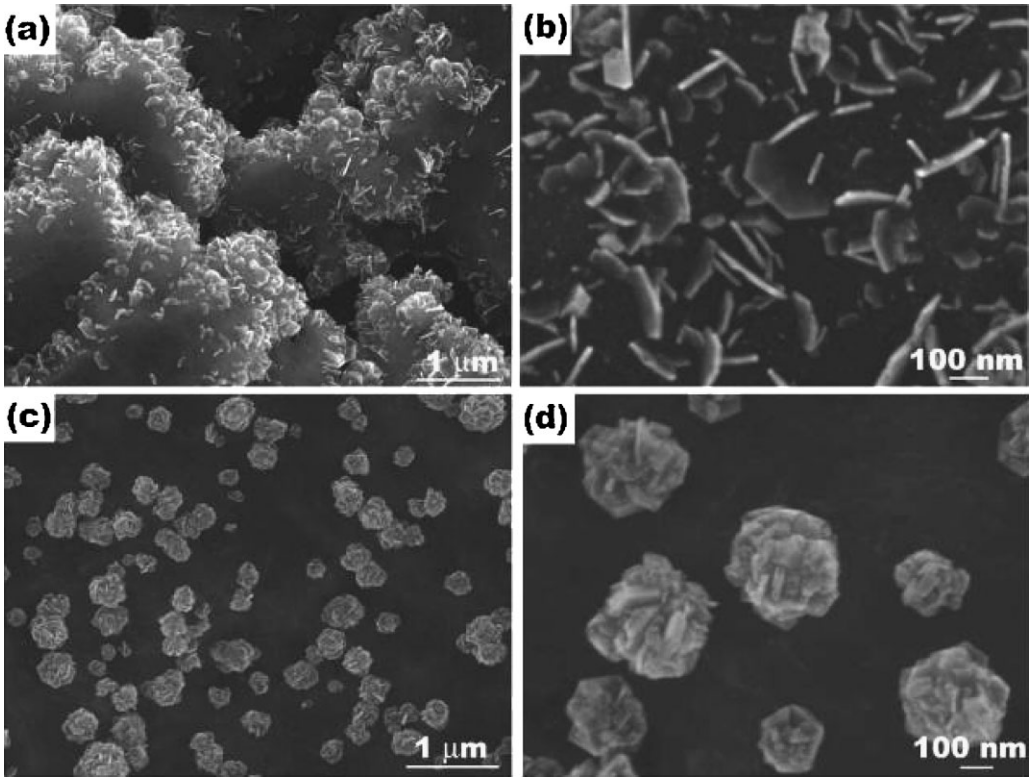

Fig. 2. a) Low magnification SEM image showing the slurry-like matrix in the region where the substrate was immersed in the plasma ball center. b) Enlarged view showing the nanoplatelets which exhibit regular hexagon-like morphology with several tens of nanometers thickness. c) SEM image of a low-temperature region showing several clusters. d) Highly magnified image showing that the clusters contain many irregular platelets.

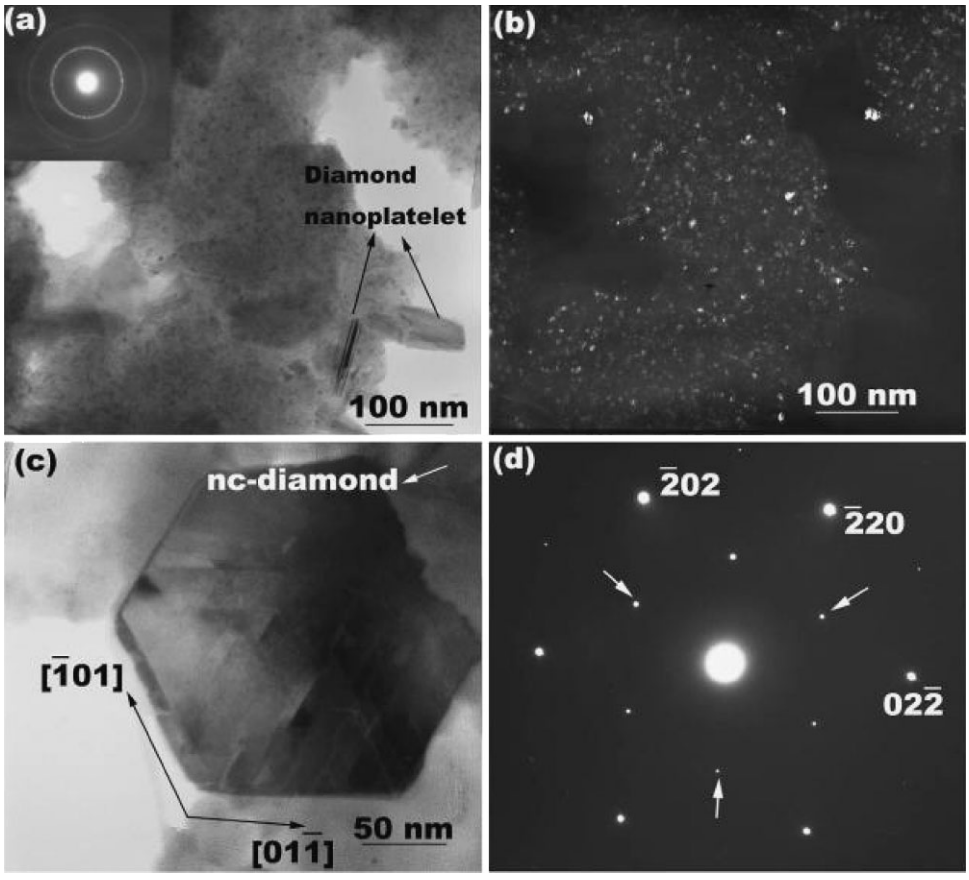

Fig. 3. a) Bright field TEM image of slurry-like matrix with some nanoplatelets. The inset shows the corresponding electron diffraction pattern showing ring pattern characteristics due to nc-diamonds. b) Dark field TEM image showing the grain size of the nc-diamonds in approximately several tens of nanometers. c) Bright field TEM image of a hexagonal platelet, and d) electron diffraction pattern of the platelet in diamond ⟨111⟩ zone axis.

of samples in an MPCVD reactor. Furthermore, we also examined the effects of various processing parameters, such as methane concentration, microwave power, and gas pressure on the growth of diamond nanoplatelets. A detailed growth mechanism is proposed and discussed.

2. Results and Discussion

Deposition of diamond nanoplatelets was carried out with three types of sample placements. Details of the method for sample placements are given in the Experimental Section. The growth parameters for the synthesis of diamond nanoplatelets are summarized in Table 1.

2.1. Growth on Au-Ge Alloy Substrate

The diamond deposition on Au-Ge alloy substrates was performed by using the sample placement I route, as shown in Figure 1a. Scanning electron microscopy (SEM) images of a slurry-like morphology can be clearly observed in the region where the substrate was immersed, close to the center of the plasma ball and near the tantalum electrode (Fig. 2a). The detailed morphologies of nanoplatelets can be observed in high-magnification SEM images (Fig. 2b). Many nanoplatelets are seen to grow on the slurry-like matrix. A lot of nanoplatelets exhibit regular faceting. Several platelets have a hexagon-like shape. The platelet length is approximately 150 nm and the thickness is about 10∼20 nm on average. The aspect ratio of the nanoplatelets is in the range ∼7–15. In addition, several small clusters can also be found at the rest region of the sample, away from the plasma ball center. Many platelets with irregular facets are found in these clusters (Figs. 2c–d).

Further characterization of the microstructure of the platelets was carried out using TEM. Figure 3a shows a bright field image of the slurry-like matrix and nanoplatelets. The inset is the corresponding selected-area electron diffraction (SAED) pattern of the slurry-like matrix. The diffraction feature in a ring pattern indicates polycrystalline characteristics. The measured d-spacings are consistent with those of cubic diamond crystal. According to the dark field image (Fig. 3b), the cluster consists of nc-diamonds of an averaged grain size of several tens of nanometers. Figure 3c shows a typical bright field image of a nanoplatelet with the corresponding electron diffraction pattern which exhibits characteristic reflections of single-crystalline diamond in the ⟨111⟩ zone axis. Based on the diffraction pattern (see Fig. 3d), each edge of the diamond nameplates is along the ⟨110⟩ direction, and the tabular plane is parallel to the {111} face. In addition to diamond diffraction spots in the pattern, as indicated by white arrows, a set of weak diffraction spots exhibit six-fold symmetry. The positions correspond to $1/3\{\bar{4}22\}$ forbidden reflections which are contributed by twins or atomic surface steps. Such diffraction phenomena have been often found in other flat crystals with face-centered cubic (fcc) structures.[19–21] In addition, some twin feature can also be observed from the bright field image (Fig. 3c). Note that the EDS elemental analysis indicates no detectable Au and Ge signals from the nc-diamond matrix and diamond nanoplatelets.

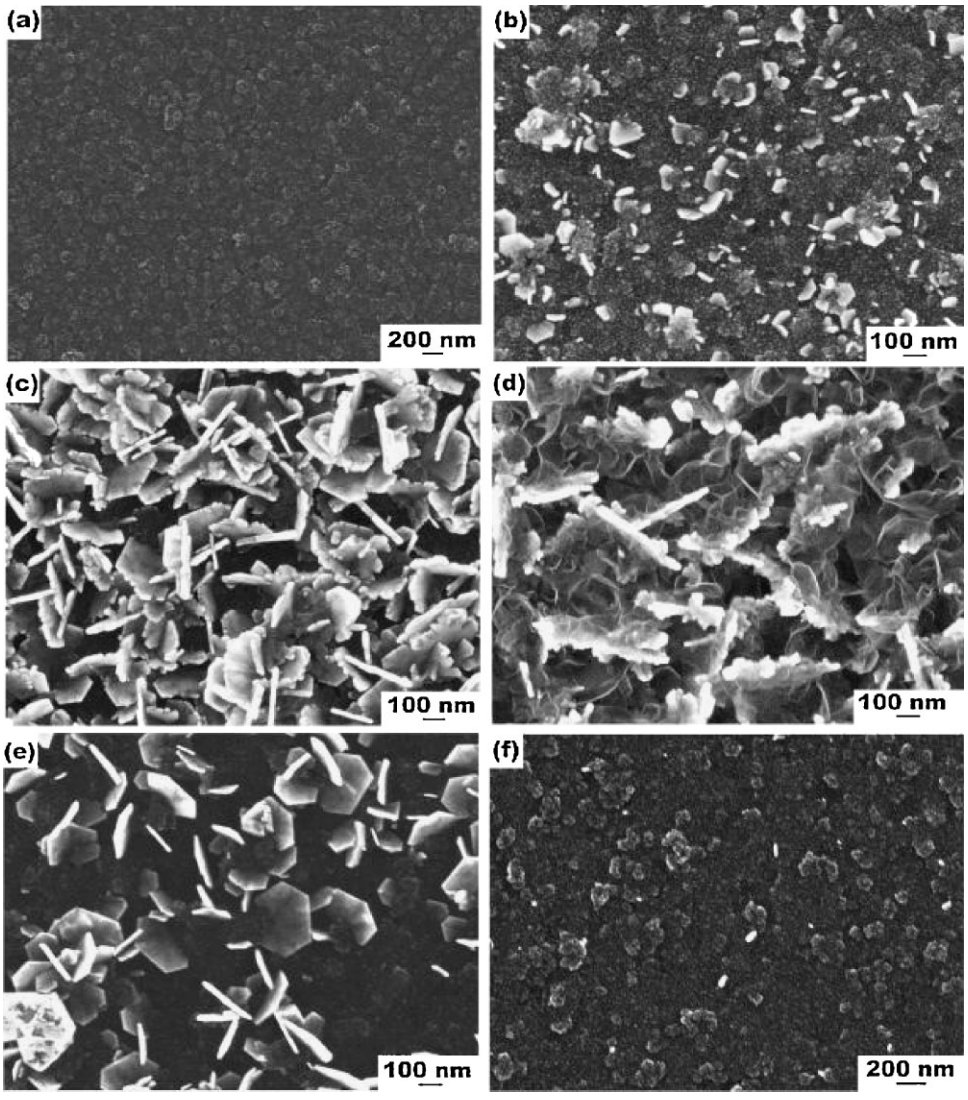

Fig. 4. a) SEM image of nc-diamond substrate. Diamond nanoplatelets grown on nc-diamond substrates through immersing sample in plasma with microwave power of 800 W and CH_4 concentration of, b) 0.667%, c) 1%, and d) 2%, respectively. e) Well-defined hexagonal diamond nanoplatelets grown on nc-diamond under microwave power 900 W and CH_4 concentration of 1%. f) The suppressed growth of diamond nanoplatelets under higher growth pressure (25 Torr) and temperature (>1150 °C).

It was noticed that diamond nanoplatelets and nc-diamonds can also grow directly on bare silicon substrates. The distribution of nanoplatelets and nc-diamonds on a bare silicon substrate may not be uniform. A high density of diamond nanoplatelets exist only on a narrow area where the temperature is high and covered by the glow plasma discharge during the application of the negative bias on the substrate. As shown for the diamond nanoplatelets grown on Au-Ge substrates, similar results can also be seen on the bare silicon substrate, so the Au-Ge alloy is unlikely to be an essential factor for the growth of diamond nanoplatelets. However, a large quantity of regular hexagonal diamond nanoplatelets are easily found on Au-Ge alloy substrates in a larger area compared with the case of diamond growth on Si substrates.

On the other hand, the formation of nc-diamond, accompanying the diamond nanoplatelet growth, is often observed. Thus, high growth temperature and nc-diamonds might be necessary for the formation of diamond nanoplatelets. Based on the above observations, the formation of nc-diamond only occurs at the regions covered by the intensive plasma discharge during the bias-enhanced nucleation (BEN) pretreatment. Therefore, such intense ion bombardment during the BEN stage could promote the diamond nucleation which results in the nc-diamond growth. Finally, the diamond nanoplatelets are only grown on the region covered with nc-diamonds.

2.2. Growth on nc-Diamond Substrates by Raising the Sample into the Plasma Ball

In order to clarify the role of nc-diamonds on the growth of diamond nanoplatelets, we employed nc-diamond films with a size of 5 mm × 5 mm as substrates for diamond nanoplatelet growth. The sample was raised close to the center of the plasma ball and fully enveloped by the plasma ball, as shown in Figure 1b. Although there have been other works which have discussed the diamond growth process through immersing substrates into plasma, studies on the growth by raising nc-diamond substrates into the plasma ball have been rare.

Figure 4a shows that the typical morphology of the nc-diamond film exhibits a non-faceted structure. The growth of diamond nanoplatelets was carried out using placement II. During growth, no BEN pretreatment was employed. Various CH_4 concentrations in hydrogen with varying plasma power were tried in order to examine their effects on platelet formation. The growth pressure was kept under 20 Torr. With low methane concentration (0.667%) at 800 W, regular, hexagon-like diamond nanoplatelets of a size of ~100 nm can be obtained (Fig. 4b). Many diamond

nanoplatelets uniformly grown on nc-diamond substrates can be achieved by immersing the nc-diamond substrates into the plasma ball. The size of diamond nanoplatelets increases with the methane concentration. However, using a higher methane concentration leads to the formation of diamond nanoplatelets with an irregular, saw-like appearance on their edges, as shown in Figure 4c. A substance with a silk-like appearance accompanying the diamond nanoplatelets can be seen for a deposition with 2% methane concentration (Fig. 4d). Based on other reported studies, this substance might be related to sp^2 carbon materials.[22]

Although the growth rate of diamond nanoplatelets can increase with increasing methane concentration, the morphology of the nanoplatelets has irregularly facetted features, which may result from strong secondary nucleation under the high methane concentration condition. In comparison with the sample grown under lower plasma power (Fig. 4c), larger diamond nanoplatelets with well-faceted appearance can be obtained with 1% methane concentration (Fig. 4e) when the plasma power is increased to 900 W. It is possible that higher input power causes the increase of temperature and the density of atomic hydrogen in the plasma which can suppress the formation of sp^2 carbon and defective diamond crystallites. From the above results, a large quantity of diamond nanoplatelets with regular hexagon-like shape can be uniformly grown on whole nc-diamond substrates under conditions of sufficient growth temperature and appropriate methane concentration. However, the growth of diamond nanoplatelets would be suppressed with a further increase of gas pressure to 25 Torr (Fig. 4f). The intensive plasma etching under such a high-temperature plasma environment (>1150 °C) may be the main reason for the slow growth rate of diamond nanoplatelets.

2.3. Growth on nc-Diamond Substrates by using the Regular Sample Placement

The plasma conditions near the center region, for instance, high growth temperature and/or high plasma density, might be just appropriate for diamond nanoplatelet growth. Such conditions might play a significant role in diamond nanoplatelet growth. Although the high temperature condition can be achieved by simply immersing a sample into the plasma ball, the distribution of active species and radicals in microwave plasma varies with the position in the plasma ball, due to the complicated variety and non-uniform nature in microwave plasma, which limits the sample size (5 mm × 5 mm) for diamond nanoplatelet growth. However, a similar plasma condition can be simply achieved by increasing plasma power and pressure. Therefore, in order to evaluate the feasibility of diamond

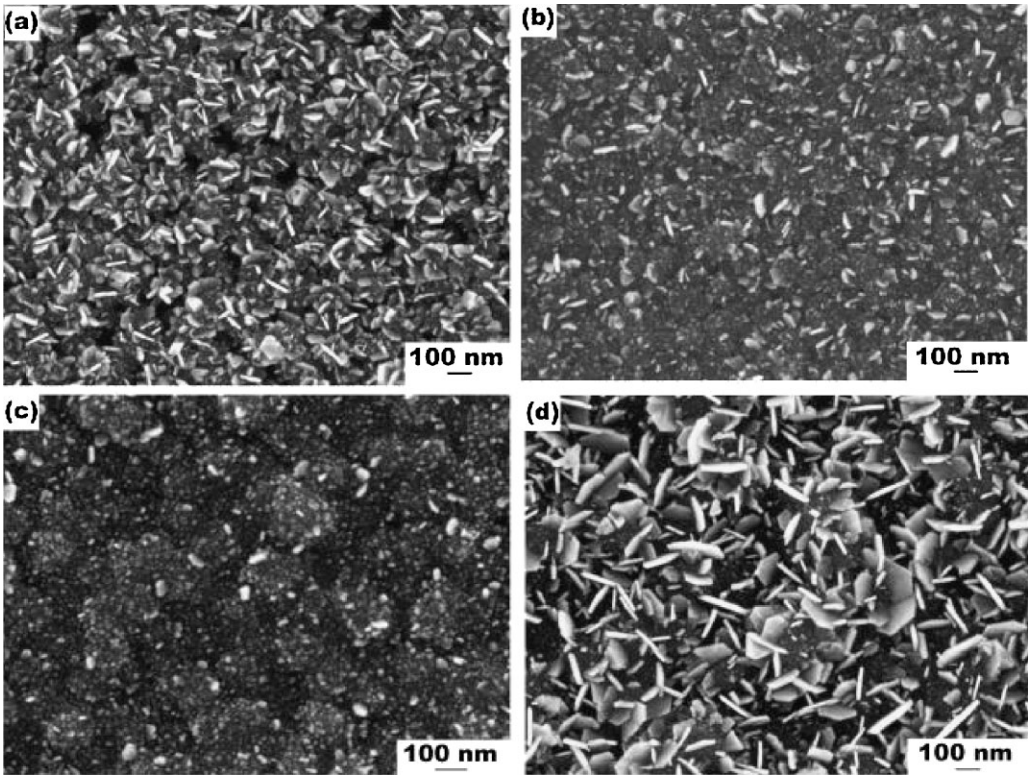

Fig. 5. Growth of diamond nanoplatelets using the regular sample placement with CH_4 concentration of 1% under pressure of, a) 50 Torr, b) 60 Torr, and c) 70 Torr. d) Well-faceted diamond nanoplatelets grown under 70 Torr with 1% CH_4 concentration conditions for extended growth duration (30 min).

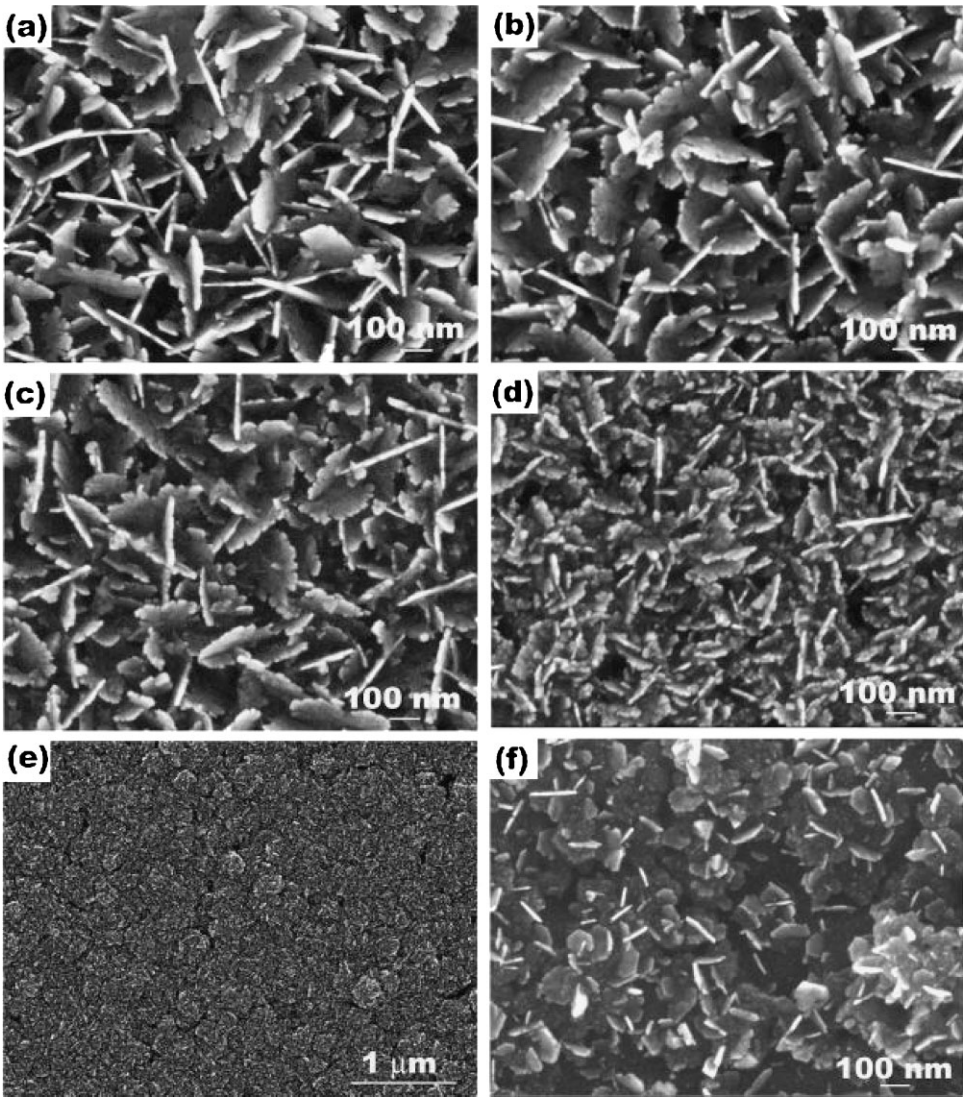

Fig. 6. Growth of diamond nanoplatelets using the regular sample placement with CH_4 concentration of 3% under pressure of, a) 70 Torr, b) 60 Torr, c) 50 Torr, d) 40 Torr, and e) 30 Torr. f) Diamond nanoplatelets with well-faceted appearance grown with 3% CH_4 concentration under 60 Torr for short growth duration of 5 min.

nanoplatelet growth without immersing a sample into the plasma ball, the growth of diamond nanoplatelets was carried out using the regular sample placement, placement III, as shown in Figure 1c. The high deposition temperature for diamond nanoplatelet growth was achieved by increasing the pressure and microwave power transmitting into the reactor cavity, instead of immersing the substrate into the plasma center. It was noticed that the deposition temperature (~1035–1150 °C) can easily be controlled by adjusting the process pressure (~30–70 Torr). In this way, the effects of CH_4 concentration and pressure on the diamond nanoplatelet growth are then shown.

Figure 5 shows diamond nanoplatelets grown under low methane concentration (1%) and various process pressures (~50–70 Torr). After 15 min growth, many diamond nanoplatelets uniformly distributed on the whole nc-diamond substrate (about 1cm × 1 cm) can be obtained, as shown in Figure 5a. The density and size of diamond nanoplatelets are reduced with increasing pressure, as shown in Figures 5a–c, similar to the case of diamond nanoplatelets grown by immersing the sample into the plasma ball. The growth rate of diamond nanoplatelets decreases with increasing pressure and temperature. Hence, the formation of a large number of diamond nanoplatelets with well-faceted appearance and of a reasonable size requires longer growth duration (30 min) under high pressure (70 Torr), as shown in Figure 5d. For the higher methane concentration condition (3%), whether diamond nanoplatelets grow under high or low pressure, the appearance of the nanoplatelets exhibits irregular faceted morphologies (Figs. 6a–d). However, there were none of the silk-like substances which were observed on the sample grown by immersing the sample into plasma under the high CH_4 concentration condition (Fig. 4d). It is noteworthy that the diamond nanoplatelets exhibit greater defective morphology under low growth pressure (see Fig. 6d). When the pressure is reduced further (30 Torr), no nanoplatelets can be found on the sample (Fig. 6e). The low growth temperature (below 1050 °C) is possibly responsible for the disappearance of diamond nanoplatelets. Similarly, the diamond nanoplatelets grown under higher methane concentration can have a higher growth rate but with the defective morphologies. It is found that the diamond nanoplatelets with well-faceted appearance can also be obtained with high CH_4 concentration for a growth duration shortened from 15 to 5 min, as shown in Figure 6f. Therefore, high microwave power and growth pressure can also lead to the increase in plasma temperature and plasma density, similar to the conditions near the plasma ball center. As a result, a large number of diamond nanoplatelets with well-faceted morphologies can be widely

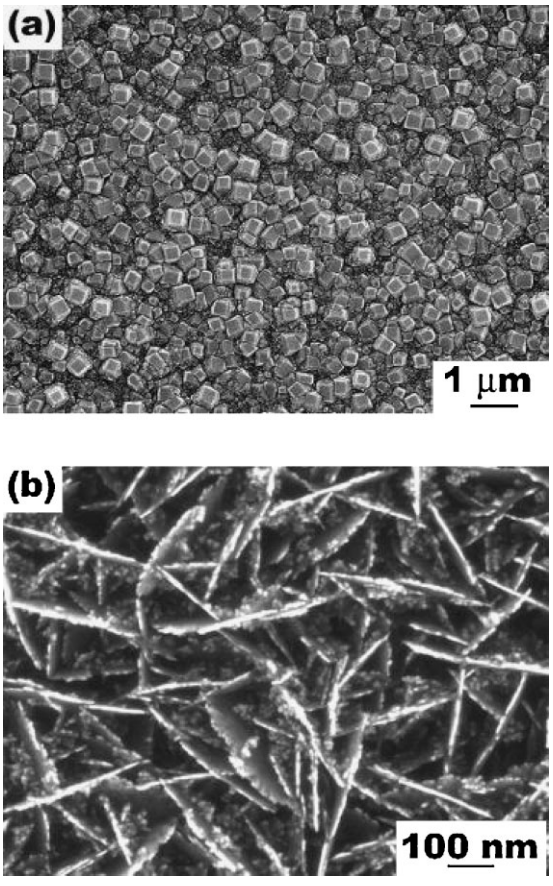

Fig. 7. a) SEM image of ⟨100⟩ texture diamond film substrate. b) Diamond nanoplatelets grown under conditions: 7% CH_4 and 2% N_2 in H_2 with power of 1000 W, and pressure of 100 Torr.

distributed over nc-diamond substrates using the regular sample placement.

Our more recent results show that similar diamond nanoplatelets can be obtained on <100> textured diamond films (Fig. 7a) when 2% nitrogen is added into the mixture of methane and hydrogen under 80–100 Torr with 800–1000 W power. A typical morphology of the platelets is shown in Figure 7b. The detailed conditions for diamond platelet formation with the addition of nitrogen need further study.

2.4. TEM Characterization of Diamond Nanoplatelets Grown on nc-Diamonds

These samples were also examined by Raman spectroscopy. However, due to the fact that the platelets were grown on diamond substrates, it is not easy to determine whether the Raman signal was from the diamond substrate, the platelets, or both. In order to directly identify the nanoplatelets grown on nc-diamond, the sample shown in Figure 5d was characterized by TEM in cross-section. Figure 8a is a bright field image revealing many nanoplatelets directly grown on the nc-diamond film. From the image, nanoplatelets exhibit various diffraction contrasts due to different orientations. The insets in Figure 8a show the SAED patterns of the nc-diamond substrate and one of the nanoplatelets. The diffraction pattern of the nanoplatelet verifies that the nanoplatelet grown on nc-diamond has single-crystalline diamond characteristics. The dark field image indicates a nc-diamond film with average grain size of several nanometers, as shown in Figure 8b. However, the sp^2 (amorphous carbon or graphite) layers accompanying the formation of these diamond platelets were also verified by electron energy loss spectroscopy (EELS) and HRTEM analysis. HRTEM and EELS characterization of diamond nanoplatelets grown under various growth conditions and by using various sample placements have been shown elsewhere.[9,13–15] Based on Raman spectroscopy and TEM analysis, sp^2 and sp^3 carbon coexist on all of the samples. However, the major component of nanoplatelets is diamond, as verified by TEM characterization.

Simultaneously, the side face structure of diamond nanoplatelets also can be observed on the same TEM specimen. The exploration of the side face structure of the diamond nanoplatelet is important in understanding the growth mechanism of diamond nanoplatelets. Figure 8c shows that one of the diamond nanoplatelets (thickness 10 nm) grown on the nc-diamond film is viewed in edge-on direction by tilting the TEM specimen. The corresponding electron diffraction pattern as shown in the inset indicates the typical twinning characteristics of diamond in ⟨110⟩ orientation. In addition to the diamond diffraction spots from the platelet, the ring patterns that are contributed from the nc-diamond film substrate can also be found. According to the diffraction pattern, the tabular plane of the diamond nanoplatelet is {111} face. From the bright field image, the twin lamellae (thickness of approximately 5 nm) are parallel to the platelet. The lateral growth mechanism for the formation of diamond nanoplatelets is closely related with this multi-parallel twin structure. An HRTEM image of the side-face structure of the platelet is shown in Figure 8d. Noting that, in our case, the side-face structure is the ridge-and-trough structure consisting of {100} and {111} faces. Such {100}/{111} ridge-and-trough side-face structures usually occur in noble metals or silver halides tabular twinned crystallites and were verified as a self-perpetuating step source for lateral growth, resulting in the anisotropic growth for tabular crystallite development.[21,23–25] The detailed lateral growth mechanism of a diamond nanoplatelet with {100}/{111} ridge-and-trough side faces adjacent to twinned planes has been discussed in our previous work.[13]

In this study, we show that the hexagon-like diamond nanoplatelets can grow on the Au-Ge alloy substrates. These diamond nanoplatelets are found to be associated with nc-diamonds grown in the high temperature region where it is immersed in the plasma ball. Similarly, hexagon-like

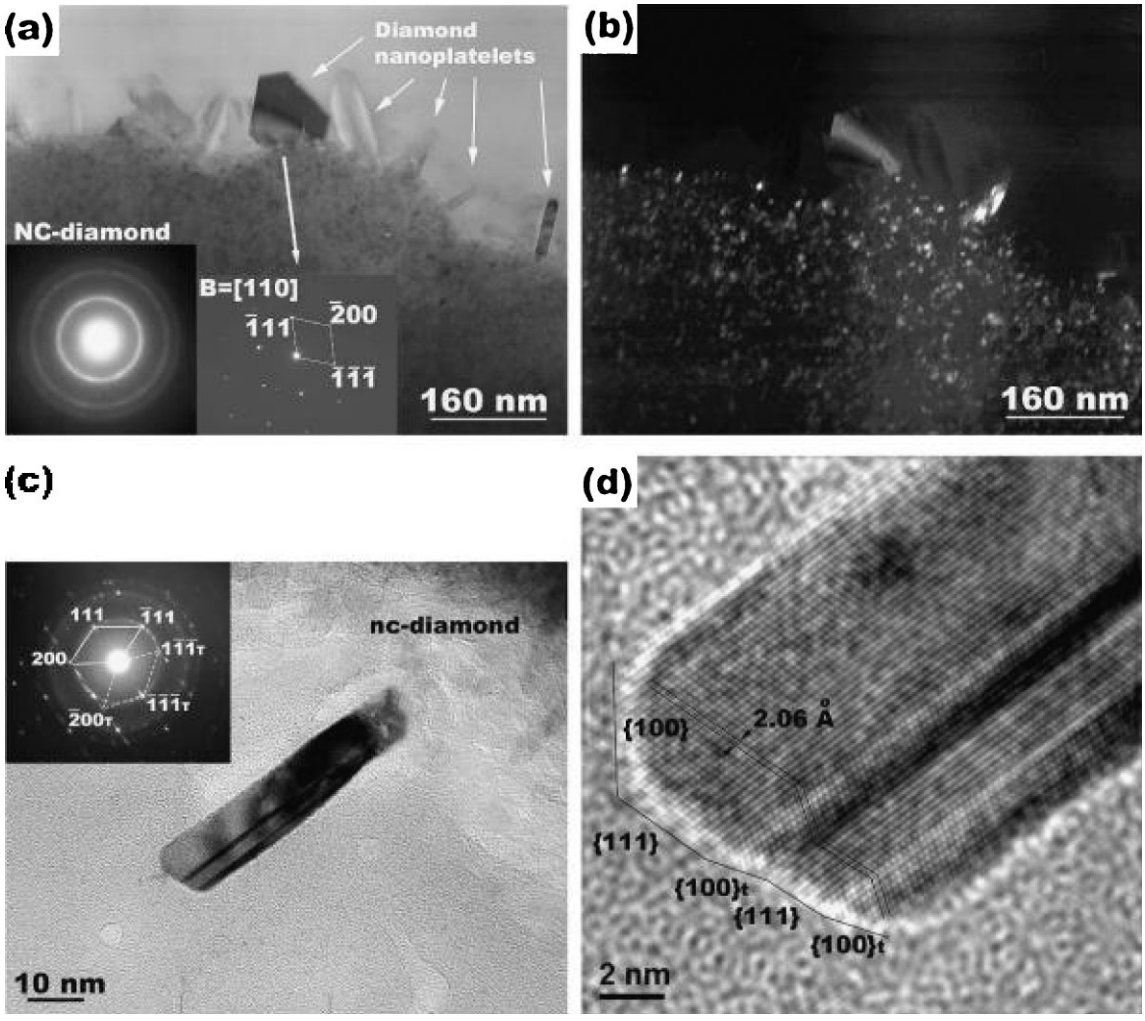

Fig. 8. a) Cross-sectional, bright field TEM image of diamond nanoplatelets grown on nc-diamond film substrate. The inset shows the electron diffraction pattern of nc-diamond and diamond nanoplatelet. b) Dark field image showing the diamond nanoplatelets and nc-diamonds. c) Bright field image of a diamond nanoplatelet viewed in the edge-on direction. The inset shows the SAED pattern of diamond nanoplatelet with ring reflections of nc-diamonds. The [01$\bar{1}$] zone-axis electron diffraction of the diamond nanoplatelet exhibiting twin characteristics. The solid lines represent diffraction spots of the matrix, and the dashed lines represent the diffraction spots of twins. d) HRTEM image showing the detailed side-face structure of the diamond nanoplatelet in ridge-and-trough edge shape consisting of {111} and {100} faces.

diamond nanoplatelets can also grow on nc-diamond film substrates in similar CVD conditions. High growth temperature (>1050 °C) and a nc-diamond seed layer are common factors for the growth of diamond nanoplatelets on both substrates at various sample placements. A large quantity of diamond nanoplatelets with well-faceted hexagon-like appearance can be obtained under appropriate CH_4 concentration and growth temperature. From cross-sectional TEM observations, it is evident that diamond nanoplatelets contain multi-parallel twins. Therefore, the anisotropic growth of a nanoplatelet is closely related with multiple parallel twin structure. The nc-diamond films contain a high defect density, especially twins, so these twins in nc-diamonds might provide a route for diamond nanoplatelet growth. Although there is no clear explanation of the relationship between high temperature plasma and the growth of diamond nanoplatelet, the atomic model of the diamond growth might provide a clue for interpretation. According to the atomic simulation,[24,26] the growth on flat {111} plane requires three carbon atoms to form a stable nucleus. Under a high temperature and intensive plasma environment, the adsorbed hydrocarbon radical on diamond {111} plane is easily abstracted by atomic hydrogen before these radicals bond together to form a stable nucleus, retarding the two-dimensional nucleation on the flat {111} plane and resulting the in slower growth rate normal to tabular {111} plane. In contrast, the higher growth rate can occur on the {100}/{111} ridge-and-trough side face of a diamond nanoplatelet, such that the anisotropic growth forms the tabular structure.

3. Conclusion

In this study, we have grown regular hexagon-like diamond nanoplatelets of 10 nm thickness on Au-Ge alloy and nc-diamond film substrates. According to electron diffraction analysis, the diamond nanoplatelet is of single crystallinity with top and bottom tabular planes in {111}. The multi-parallel twins in diamond platelets have been revealed by cross-sectional TEM observations. The side faces consisting of {100}/{111} trough-and-ridge edge structure enhance the growth rate in the lateral direction. The highly defective nc-diamonds provide a growth route for the formation of diamond nanoplatelets. The propagation of the diamond nanoplatelet closely relates to the intensive chemical reaction resulting from high temperature plasma.

4. Experimental

The Au-Ge alloy substrates were prepared as follows: Before deposition of Au/Ge layers, a 200 nm thick SiO_2 intermediate layer was deposited on a Si(100) substrate by plasma-enhanced (PE)CVD. Germanium and gold films were deposited in sequence by the electron beam evaporation method. The thickness of the germanium and gold layers was 65 and 130 nm, respectively, and the thickness ratio corresponded to 12wt.-% Ge composition which would allow them to form a liquid Au-Ge alloy during PECVD conditions for diamond growth. A nc-diamond film of 200 nm thickness was deposited on a Si(100) single-crystal substrate by MPCVD. During nc-diamond film deposition, 200 V negative bias was applied to the substrate to enhance diamond secondary nucleation. The CH_4 concentration in H_2 was 3% in volume, and the pressure was kept at 20 Torr during the deposition period.

Deposition of diamond nanoplatelets was carried out in a 2.45 GHz ASTeX-type MPCVD reactor. The three types of sample placement for diamond nanoplatelet growth employed in this study are schematically illustrated in Figure 1. The Au-Ge substrates (1 cm × 1 cm) were immersed vertically in the microwave plasma, as shown in Figure 1a. A tantalum wire acted as a counter electrode and was connected to the grounded chamber wall, so that the substrate could be negatively biased. For diamond nanoplatelets grown on nc-diamond substrates, the nc-diamond substrates (size 5 mm × 5 mm) were placed on a molybdenum holder raised close to the center of the plasma ball, as shown in Figure 1b. During diamond nanoplatelet growth, no BEN pretreatment was employed. In addition to the above conditions, diamond nanoplatelets were also synthesized with regular sample placement without immersion of samples in the plasma ball, as shown in Figure 1c. The substrate temperature was monitored by a single-color optical pyrometer.

After deposition, the surface morphology was examined using a field-emission SEM (JEOL JSM-6500F at 10 kV). The nanoplatelets were further characterized by TEM. A Philips Tecnai 20 TEM was employed for image observation and SAED analyses. Furthermore, in order to analyze the details of the microstructure of diamond nanoplatelets, HRTEM was performed on a JEOL-2010F microscope with an information limit of 0.10 nm. TEM specimens were thinned by a conventional mechanical process, followed by Ar^+ ion beam milling.

Received: November 3, 2007
Revised: April 9, 2008

[1] D. M. Gruen, *Annu. Rev. Mater. Sci.* **1999**, *29*, 211.
[2] K. Subramanian, W. P. Kang, J. L. Davidson, Y. M. Wong, B. K. Choi, *Diamond Relat. Mater.* **2007**, *16*, 1408.
[3] J. I. Chao, E. Perevedentseva, P. H. Chung, K. K. Liu, C. Y. Cheng, C. C. Chang, C. L. Cheng, *Biophys. J.* **2007**, *93*, 2199.
[4] W. S. Yang, O. Auciello, J. E. Butler, W. Cai, J. A. Carlisle, J. Gerbi, D. M. Gruen, T. Knickerbocker, T. L. Lasseter, J. N. Russell, L. M. Smith, R. J. Hamers, *Nature Mater.* **2002**, *1*, 253.
[5] J. A. Carlisle, O. Auciello, *Interface* **2003**, *12*, 28.
[6] O. Shenderova, D. Brenner, R. S. Ruoff, *Nano Lett.* **2003**, *3*, 805.
[7] A. S. Barnard, S. P. Russo, I. K. Snook, *Nano Lett.* **2003**, *3*, 1323.
[8] A. S. Barnard, I. K. Snook, *J. Chem. Phys.* **2004**, *120*, 3817.
[9] H. G. Chen, L. Chang, *Diamond Relat. Mater.* **2004**, *13*, 590.
[10] E. S. Baik, Y. J. Baik, S. W. Lee, D. Jeon, *Thin Solid Films* **2000**, *377–378*, 295.
[11] Y. Ando, Y. Nishibayashi, A. Sawabe, *Diamond Relat. Mater.* **2004**, *13*, 633.
[12] H. Masuda, T. Yanagishita, K. Yasui, K. Nishio, I. Yagi, T. N. Rao, A. Fujishima, *Adv. Mater.* **2001**, *13*, 247.
[13] H. G. Chen, L. Chang, *J. Mater. Res.* **2005**, *20*, 703.
[14] C. A. Lu, L. Chang, *Diamond Relat. Mater.* **2004**, *13*, 2056.
[15] C. A. Lu, L. Chang, *Mater. Chem. Phys.* **2005**, *92*, 48.
[16] R. Roy, K. A. Cherian, J. P. Cheng, A. Badzian, C. Langlade, H. Dewan, W. Drawl, *Mater. Res. Innov.* **1997**, *1*, 117.
[17] P. H. Fang, L. Hou, *Mater. Res. Innov.* **2000**, *3*, 360.
[18] C. K. Kao, J. K. Yan, L. Chang, S. Y. Cho, H. G. Chen, *Diamond Relat. Mater.* **2004**, *13*, 585.
[19] S. Iijima, *Ultramicroscopy* **1981**, *6*, 41.
[20] D. Cherns, *Philos. Mag.* **1974**, *30*, 549.
[21] A. I. Kirkland, D. A. Jefferson, D. G. Duff, P. P. Edwards, I. Gameson, B. F. G. Johnson, D. J. Smith, *Proc. R. Soc. Lond. A* **1993**, *440*, 589.
[22] J. J. Wang, M. Y. Zhu, R. A. Outlaw, X. Zhao, D. M. Manos, B. C. Holloway, V. P. Mammana, *Appl. Phys. Lett.* **2004**, *85*, 1265.
[23] D. R. Hamilton, R. G. Seidensticker, *J. Appl. Phys.* **1960**, *31*, 1165.
[24] C. Angus, M. Sunkara, S. R. Sahaida, J. T. Glass, *J. Mater. Res.* **1992**, *7*, 3001.
[25] G. Bögels, T. M. Pot, H. Meekes, P. Bennema, D. Bollen, *Acta Crystallogr. A* **1997**, *53*, 84.
[26] M. Grujicic, S. G. Lai, *J. Mater. Sci.* **1999**, *34*, 7.

